Electronic Supplementary Material (ESI) for Chemical Science.

Electronic Supporting Information

Structural Modulation of Aggregation-Induced Emission Luminogen for NIR-II Fluorescence Imaging/Photoacoustic Imaging of Tumors

Xue Liu, Yonghong Tan, Jianyu Zhang, Weigeng Huang, Dingyuan Yan, Dong Wang* and Ben Zhong Tang**

Table of Contents

Experimental section

Materials

Commercially available chemicals, such as di-*p*-tolylamine, 2-bromothiophene, *t*BuONa, *n*-BuLi, Bu_3SnCl, $Pd_2(dba)_3$, $Pd(PPh_3)_4$, 4,7-dibromobenzo[*c*][1,2,5]thiadiazole, 4,9-dibromonaphtho[2,3-*c*][1,2,5]thiadiazole, 4,9-dibromonaphtho[2,3-*c*][1,2,5]selenadiazole, *etc.* were obtained from Adamas, Energy, TCI or Bide and used as received unless otherwise stated.

Instruments

^1H and ^{13}C NMR spectra were recorded with a Bruker ARX 400 NMR spectrometer using chloroform-*d* or THF-d_8 as solvent. UV-Vis spectra were recorded anaerobically using a Shimadzu UV-1800 spectrophotometer. Size distribution was analyzed on a dynamic light scattering (DLS) using a Malvern Zeta sizer Nano ZSP. Particle size and morphology were observed on a HITACHI-HT7700 transmission electron microscope. The cellular fluorescence images were taken by a confocal laser scanning microscope (CLSM, ZEISS-LSM900). The cell viability was detected by CCK-8 kit and MTT, and the absorbance of each sample was measured at 450 nm and 490 nm, respectively, using a microplate reader (synergyH1, BioTek). The in vivo fluorescence imaging was carried out on a commercial NIR-II in vivo imaging system (MARS-HS, Artemis Intelligent Imaging). In vivo PAI of mice were taken on Vevo LAZR (VisualSonics, Canada).

Preparation of NPs

1 mL of THF solution containing 1 mg of compound T-NSD and 5 mg of DSPE-$mPEG_{2000}$ was poured into 9 mL of deionized water, followed by sonication with a microtip probe sonicator (XL2000, Misonix Incorporated, NY) at 45% output power for 2 min continuously. Then the mixtures were transferred into dialysis tube (MWCO 3500 Da) and dialyzed against deionized water for 24 h.

Fresh deionized water was replayed every 4 h to remove the residue THF. The prepared NPs aqueous solutions were concentrated to the specified concentrations by ultrafiltration before use.

Fluorescence QY measurement

Relative fluorescence quantum yields of AIE-4PEG550 dissolved in water was measured in a similar way to a previous publication.[1] ICG was employed as the reference (QY = 1.6% in pure water). For reference calibration, a series of ICG dissolved in pure water was diluted to its absorbance value of ~0.10, ~0.08, ~0.06, ~0.04, and ~0.02 at 660 nm. The emission was collected in the transmission geometry with a 700 nm long-pass filter to reject the excitation light, and the integrated fluorescence was plotted against absorbance for both reference and samples. The quantum yield was calculated based on the equation as follows:

$$\mathrm{QY}_{\mathrm{sample(wavelength)}} = \mathrm{QY}_{\mathrm{ref}} \cdot \frac{S_{\mathrm{sample(wavelength)}}}{S_{\mathrm{ref}}} \cdot \left(\frac{n_{\mathrm{sample(wavelenth)}}}{n_{\mathrm{ref}}}\right)^2$$

Where “n” represents the refractive index, “S” represents the slopes obtained by linear fitting of the integrated emission spectra of the samples against the absorbance at 660 nm, respectively.

Cell culture and animal models

4T1 cells were cultured in 1640 culture medium, supplied with 10% FBS (Gibco), penicillin (50 U mL^{-1}, Gibco) and streptomycin (50 mg mL^{-1}, Sigma, MO, USA), and kept in a sterile and humidified incubator at 37 °C in 5% CO_2/95% air. Male Balb/c mice (5-6 weeks old) were purchased from the Beijing Vital River Laboratory Animal Technology. All the animal experiments were carried out with the regulations of the Animal Ethical and Welfare Committee of Shenzhen University (AEWC-SZU). For establishment of 4T1 tumor models, 5×10^5 4T1 cells were seeded into the flank of Balb/c mice (6-8 weeks old). Around 7 days post-injection, the mice in different groups

underwent the corresponding treatments.

Intracellular tracking

T-NSD was coated with 1,2-distearoyl-*sn*-glycero-3-phosphoethanolamine-*N*-[methoxy(polyethylene glycol)-2000] with conjugated fluorescein isothiocyanate (FITC-DSPE-$mPEG_{2000}$) to fabricate FITC-NPs. For cellular uptake and location of FITC-NPs, 4T1 cells were seeded in a 50-mm glass bottom tissue culture dish for 12 h and were incubated with FITC-NPs, 5 μg mL^{-1}) for 3 h, 6 h, 9 h, 12 h, respectively. After washing three times with PBS, cells were cultured with Nile red, Lyso-Tracker Red, Mito-Tracker Deep Red, respectively, for another 10 min at room temperature. Subsequently, cells were imaged by confocal laser scanning microscopy to detect cellular internalization of NPs.

Cytotoxicity assay

The cells were seeded in a 96-well plate with 5×10^3 cells per well and cultured for 12 h. Then the cells were treated with T-NSD NPs (0, 1, 2, 5, 10, 20, 50 μg mL^{-1}) in fresh medium at various concentrations for 24 h in the dark. After washing three times, Hela cells were incubated with fresh serum-free medium containing 10% CCK-8 (Dojindo, Kumamoto, Japan) for 2 h in the dark. In addition, 4T1 cells were added to 10% MTT medium for 4 h, and then the medium was replaced with DMSO. Then the absorbance was detected with a microplate reader to evaluate viable percentage of cells.

In vivo NIR-II excited fluorescence and photoacoustic imaging

For NIR-II fluorescent and photoacoustic imaging, the 4T1 breast tumor bearing mice were administered with 200 μL of T-NSD NPs (1 mg mL^{-1}) through tail vein. Then the *in vivo* NIR-II fluorescent images at predetermined time intervals (0, 1, 3, 6, 12, 24, 36 and 48 h) post-injection

were subsequently captured on the NIR-II in vivo imaging system with the excitation of a 660 nm laser. Besides, in vivo PAI was also carried out on the commercial optoacoustic imaging system at designated time intervals after intravenous injection of T-NSD NPs. The details of the imaging protocols for PA sequence are as follows. The photoacoustic spectrum of T-NSD NPs was obtained by recording the photoacoustic signals of 100 μg mL^{-1} T-NSD NPs injected into a transparent flexible tube ranging from 680 nm to 970 nm. The spectrum that was obtained was later used for spectral unmixing. The photoacoustic images and intensities of the tumor site with different time were obtained with 700 nm laser excitation under the same conditions. To reduce the interference of oxy/deoxy-hemoglobin and tissue, photoacoustic signals before injection were selected as control for analysis. PA spectra of T-NSD NPs were also collected for spectral analysis. After injection, mice were scanned at different time intervals. PA intensity was quantified by image analysis software, Vevo LAZR (Fujifilm VisualSonics). After spectral separation, the average photoacoustic signals of the tumor area were regarded as the PA signal intensity of T-NSD NPs. The NIR-II fluorescent and photoacoustic images at 0 h were acquired before injection of T-NSD NPs. In an attempt to evaluate the tissue distributions of T-NSD NPs, the mice were sacrificed at 36 h post-injection. Major organs (heart, liver, spleen, lung, and kidney) and tumor were excised, followed by washing the surface with PBS several times for NIR-II fluorescent imaging and quantitative analyses.

Histological assay

Main organs (heart, liver, spleen, lung and kidney) and tumors of mice were collected 7 days after T-NSD NPs (100 μg per mouse) intravenous injection for the analysis of biocompatibility. Tissues were fixed in 4% paraformaldehyde overnight, embedded in paraffin and sectioned at 5 μm thickness via cryostat. The sections were stained with H&E staining, and imaged by a digital

pathology slide scanner.

DFT calculations

Density functional theory (DFT) calculations were performed using the Gaussian 16 program packages.[1] The geometries of all compounds at ground state were fully optimized at the M06-2X/6-31G (d, p) level with the polarizable continuum model and self-consistent reaction field (solvent = DMSO). The geometries of all compounds at S_1 state were calculated using time-dependent DFT (TD-DFT) method at the same level. Reorganization energy analysis of all compounds was performed using Molecular Materials Property Prediction Package (MOMAP).[2-4]

Synthesis and Characterization

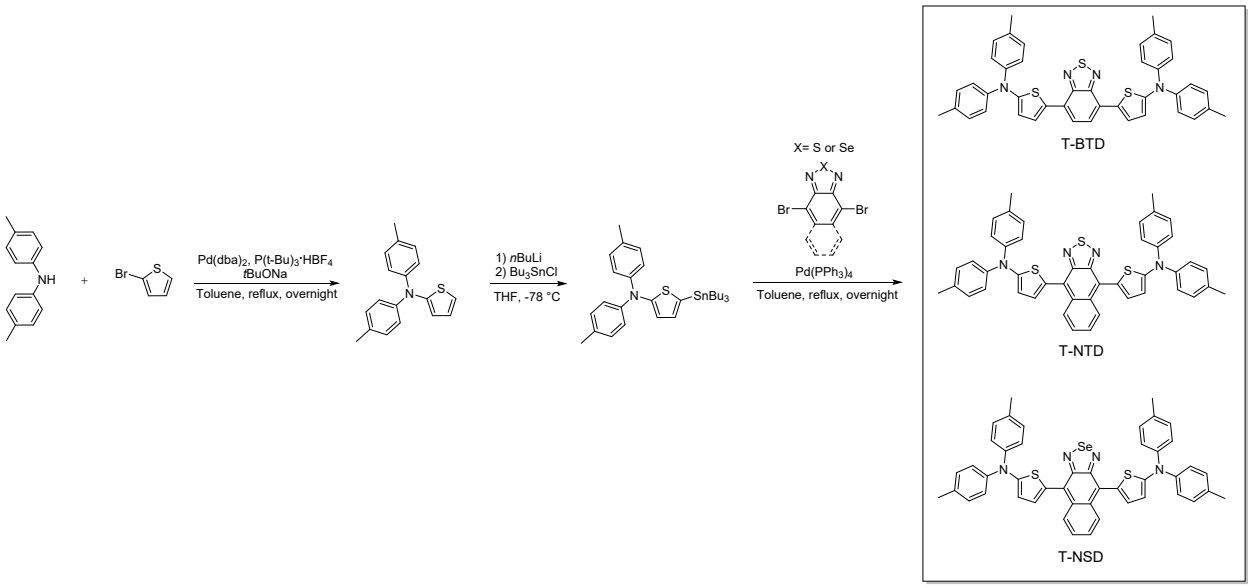

Scheme S1. The synthetic routes of T-BTD, T-NTD and T-NSD.

Synthesis of *N*,*N*-di-*p*-tolylthiophen-2-amine

N,*N*-Di-*p*-tolylthiophen-2-amine was synthesized according to the previous report.[5] Di-*p*-tolylamine (1.97 g, 10 mmol), 2-bromothiophene (1.96 g, 12 mmol), $Pd_2(dba)_3$ (0.46 g, 0.5 mmol), *tri-tert*-butylphosphine tetrafluoroborate (0.29 g, 1 mmol) and *t*BuONa (0.97 g, 10 mmol) were added into a 100 mL two-necked round-bottom flask, and the mixture was further degassed with dry nitrogen for 20 min. Then anhydrous toluene (30 mL) was added, and the mixture was heated to reflux and stirred for 12 h. After cooling down to room temperature, water was added, and the mixture was washed with dichloromethane three times. The combined organic layers were dried with Na_2SO_4, and the solvent was evaporated under reduced pressure. The resides was purified by column chromatography to afford product as a colorless solid (84% yield). **^{1}H NMR (600 MHz, Chloroform-*d*)** δ 7.03 (d, *J* = 8.7 Hz, 4H), 7.00 (d, *J* = 8.5 Hz, 4H), 6.88 (dd, *J* = 5.6, 1.4 Hz, 1H), 6.82 (dd, *J* = 5.6, 3.7 Hz, 1H), 6.62 (dd, *J* = 3.7, 1.4 Hz, 1H), 2.28 (s, 6H). **^{13}C NMR (151 MHz, Chloroform-*d*)** δ 152.42, 145.92, 132.36, 129.80, 125.90, 122.54, 120.10, 119.72, 20.87.

Synthesis of T-BTD

n-BuLi (0.5 mL, 1.2 mmol, 2.4 M in hexane) was added dropwise to a solution of *N*,*N*-di-*p*-tolylthiophen-2-amine in THF (0.28 g, 1.0 mmol, 5 mL) at -78 °C. And the reaction mixture was continued for 0.5 h at -78 °C. Then tributyltin chloride (0.43 g, 1.2 mmol) was added into the solution at one portion. After stirring the mixture for 12 h at room temperature, KF solution was added to quench the reaction. The resulting mixture was extracted with ethyl acetate for three times, the combined organic phase was dried with Na_2SO_4. After removal of the solvent, corresponding organotin intermediate was obtained and was used directly in next step.

A 5 mL tube was charged with above obtained crude product, 4,7-dibromobenzo[*c*][1,2,5]thiadiazole (88 mg, 0.3 mmol), $Pd(PPh_3)_4$ (22 mg, 0.03 mmol) and degassed dry toluene (2 mL), and sealed with a Teflon cap. The reaction mixture was heated with stirring to 120 °C overnight. Upon cooling, the crude product was quenched with KF solution and extracted with DCM. The combined organic phase was dried with Na_2SO_4. After removing the solvent, the product was purified with neutral aluminum oxide column to obtain a red solid powder (yield: 79%). **^{1}H NMR (500 MHz, Chloroform-*d*)** δ 7.93 (d, *J* = 4.1 Hz, 2H), 7.56 (s, 2H), 7.12 (q, *J* = 8.5 Hz, 16H), 6.62 (d, *J* = 4.1 Hz, 2H), 2.33 (s, 12H). **^{13}C NMR (126 MHz, Chloroform-*d*)** δ 154.19, 152.74, 145.42, 133.42, 130.99, 130.03, 127.03, 125.20, 124.38, 123.62, 118.47, 20.99.

Synthesis of T-NTD

The synthesis of T-NTD was similar with T-BTD (yield: 62%). **^{1}H NMR (600 MHz, THF-d_8)** δ 8.52 (dd, *J* = 7.0, 3.2 Hz, 2H), 7.41 (dd, *J* = 7.0, 3.2 Hz, 2H), 7.29 (d, *J* = 3.9 Hz, 2H), 7.17 – 7.13 (m, 8H), 7.10 (d, *J* = 8.5 Hz, 8H), 6.71 (d, *J* = 3.9 Hz, 2H), 2.29 (s, 12H). **^{13}C NMR (151 MHz, THF-d_8)** δ 156.53,

152.31, 146.62, 133.85, 133.24, 130.73, 130.61, 129.32, 128.00, 127.32, 124.21, 123.81, 118.42, 20.85.

Synthesis of T-NSD

The synthesis of T-NSD was similar with T-BTD (yield: 54%). **^{1}H NMR (400 MHz, THF-d_8)** δ 8.23 (dd, *J* = 7.1, 3.3 Hz, 2H), 7.16 (dd, *J* = 7.1, 3.2 Hz, 2H), 7.11 (d, *J* = 3.9 Hz, 2H), 7.01 (q, *J* = 8.6 Hz, 16H), 6.59 (d, *J* = 3.9 Hz, 2H), 2.19 (s, 12H). **^{13}C NMR (126 MHz, THF-d_8)** δ 157.22, 155.36, 145.74, 132.68, 132.44, 129.77, 129.59, 129.49, 127.31, 126.10, 123.70, 123.12, 117.56, 19.87.

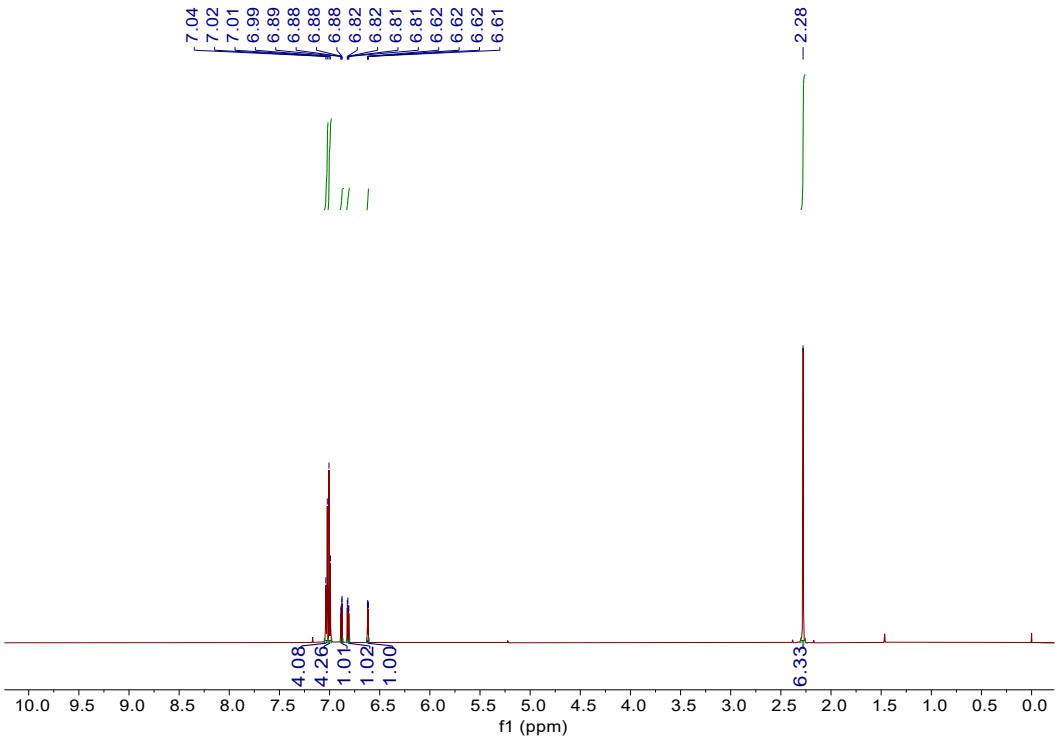

Figure S1. ^{1}H NMR spectrum of *N*,*N*-di-*p*-tolylthiophen-2-amine.

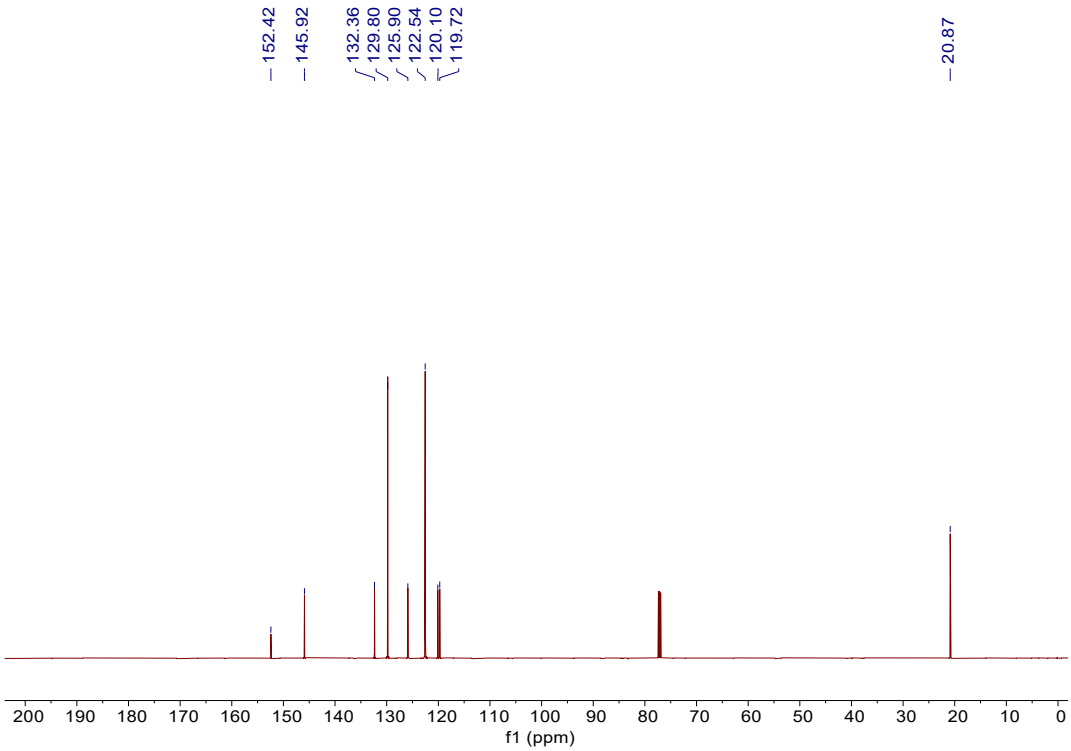

Figure S2. ^{13}C NMR spectrum of *N*,*N*-di-*p*-tolylthiophen-2-amine.

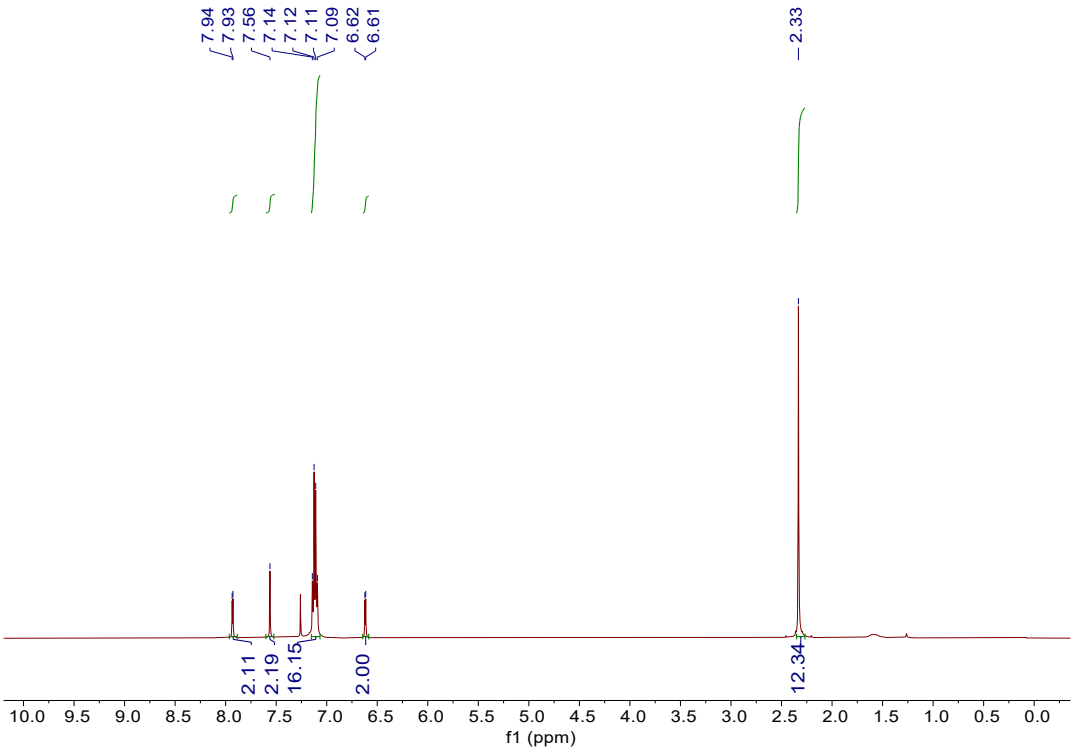

Figure S3. ^{1}H NMR spectrum of T-BTD.

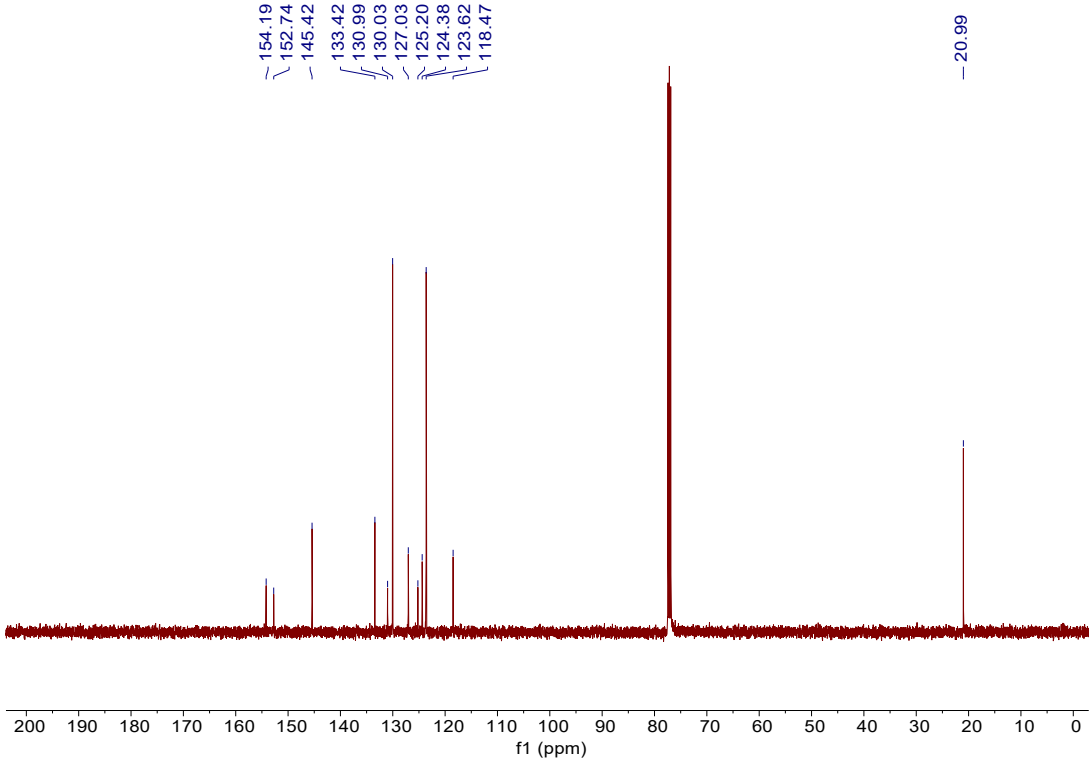

Figure S4. ^{13}C NMR spectrum of T-BTD.

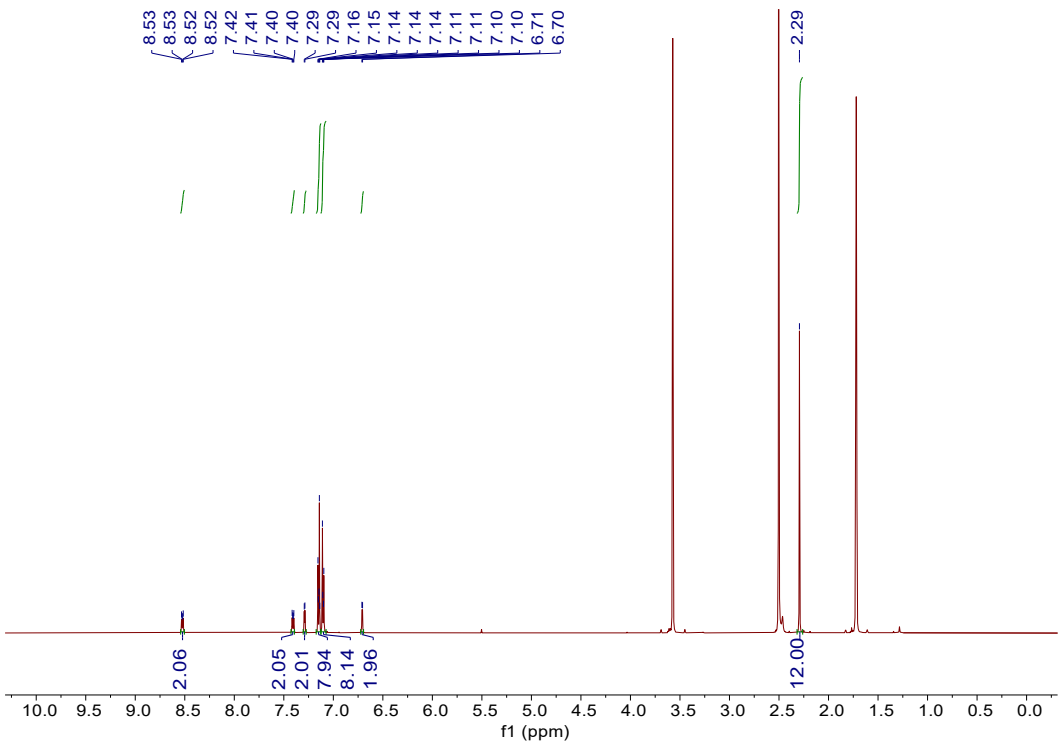

Figure S5. ^{1}H NMR spectrum of T-NTD.

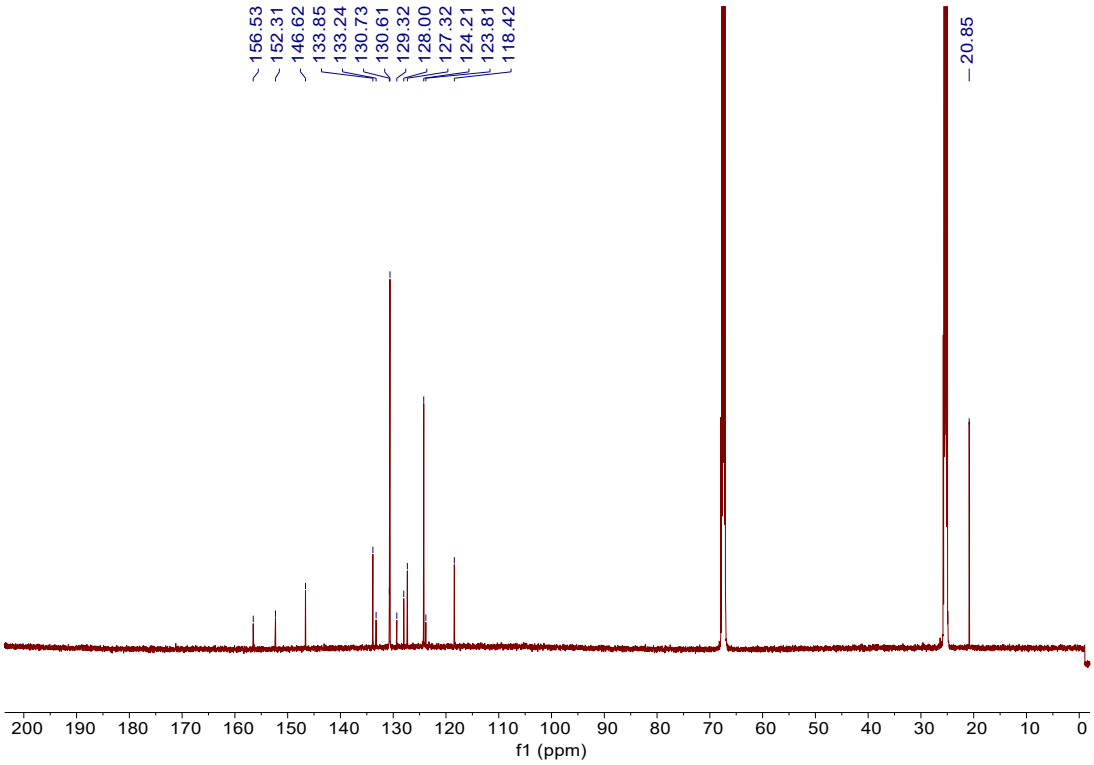

Figure S6. ^{13}C NMR spectrum of T-NTD.

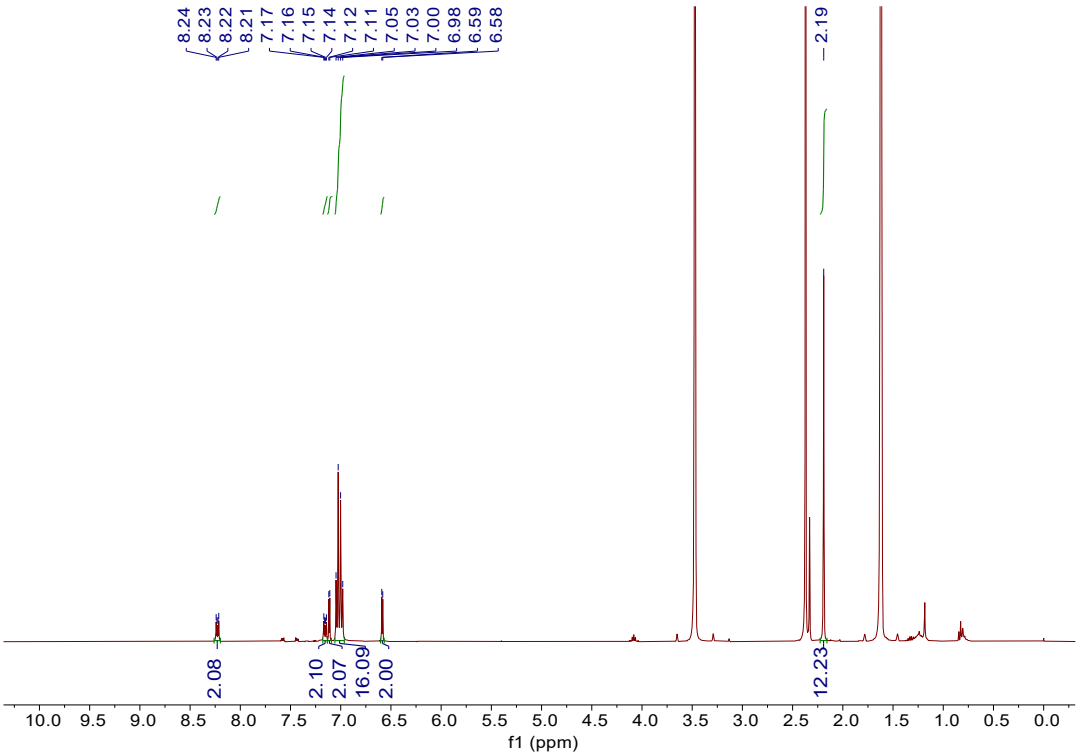

Figure S7. ^{1}H NMR spectrum of T-NSD.

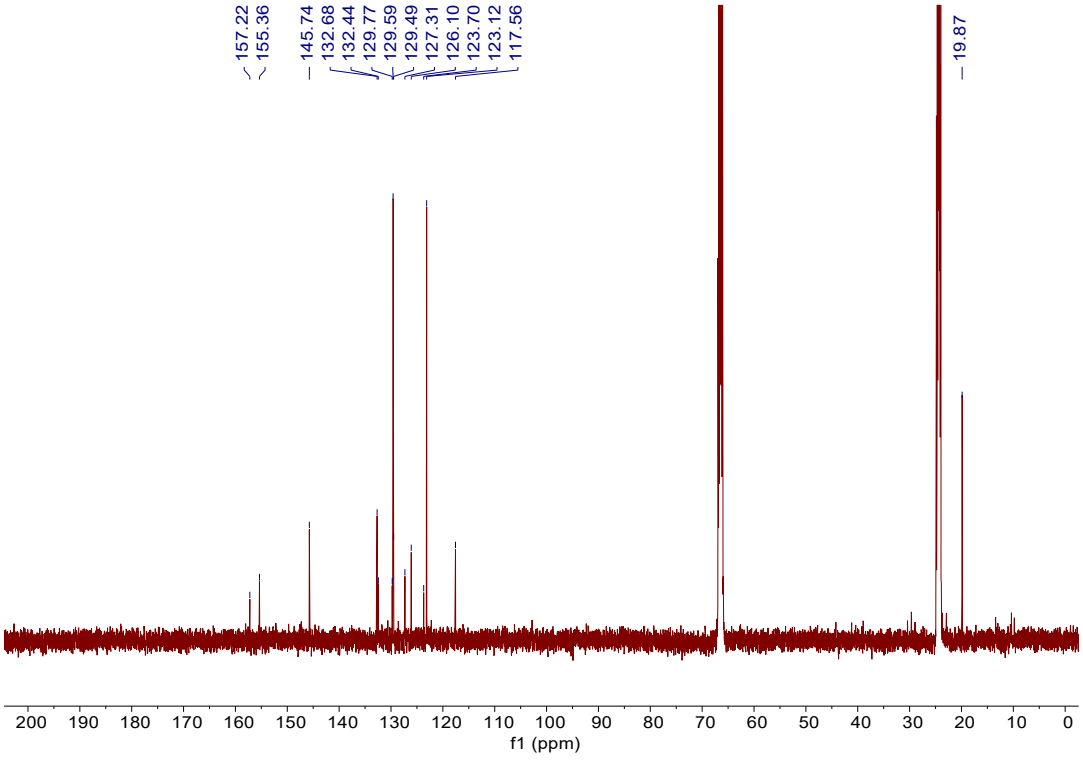

Figure S8. ^{13}C NMR spectrum of T-NSD.

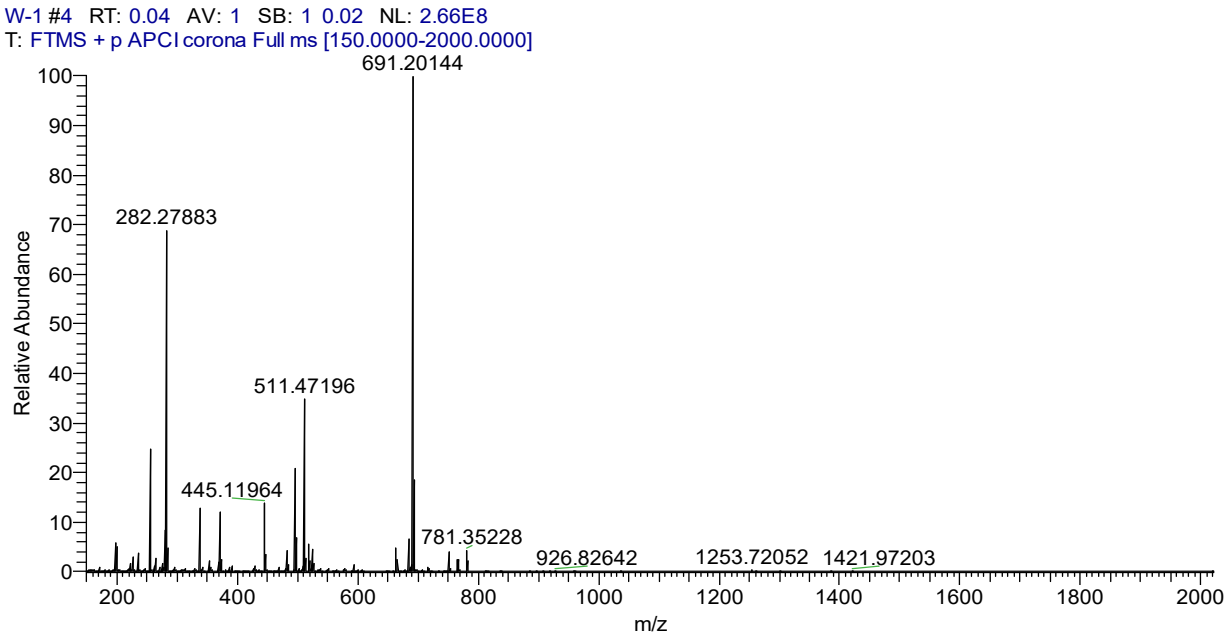

Figure S9. MS spectrum of T-BTD.

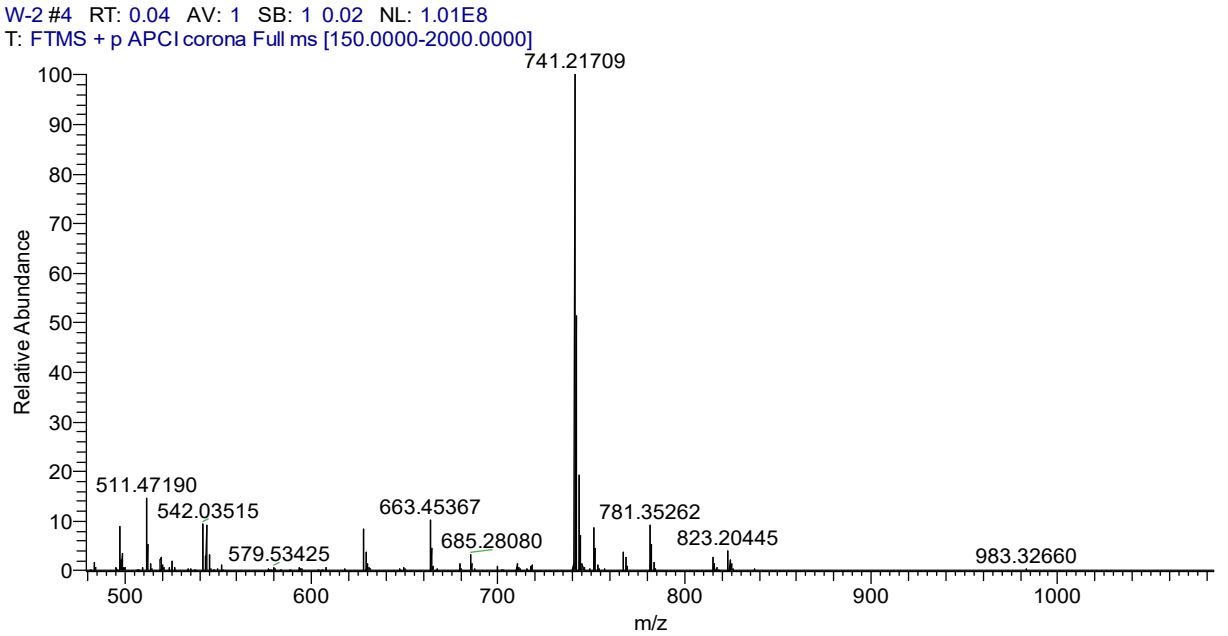

Figure S10. MS spectrum of T-NTD.

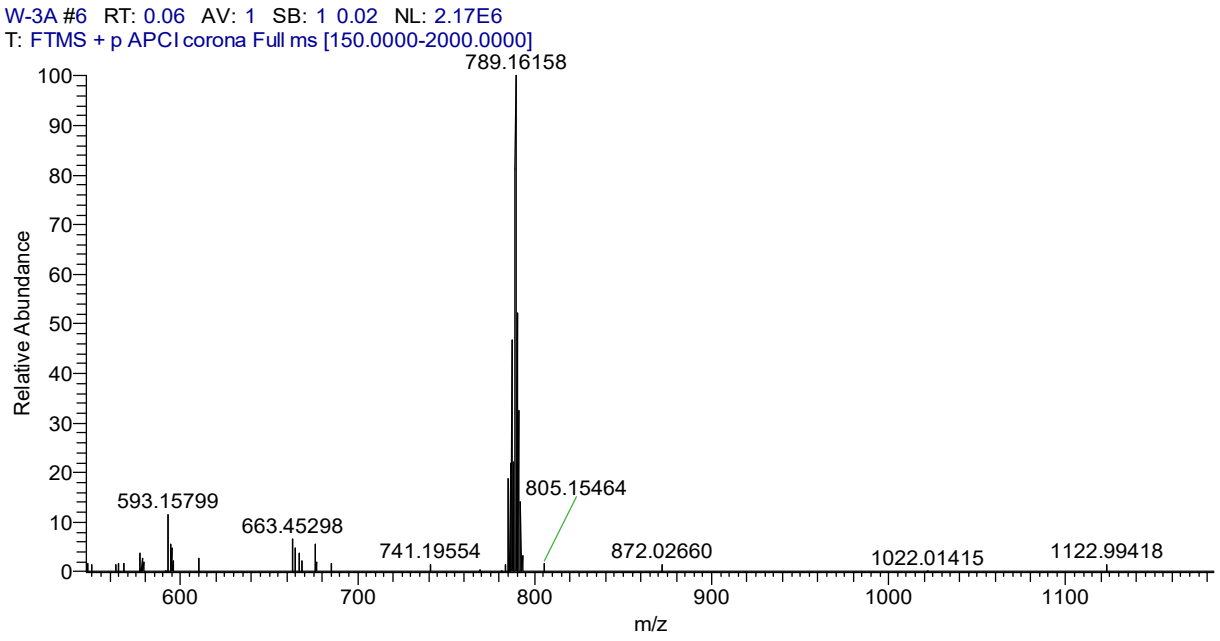

Figure S11. MS spectrum of T-NSD.

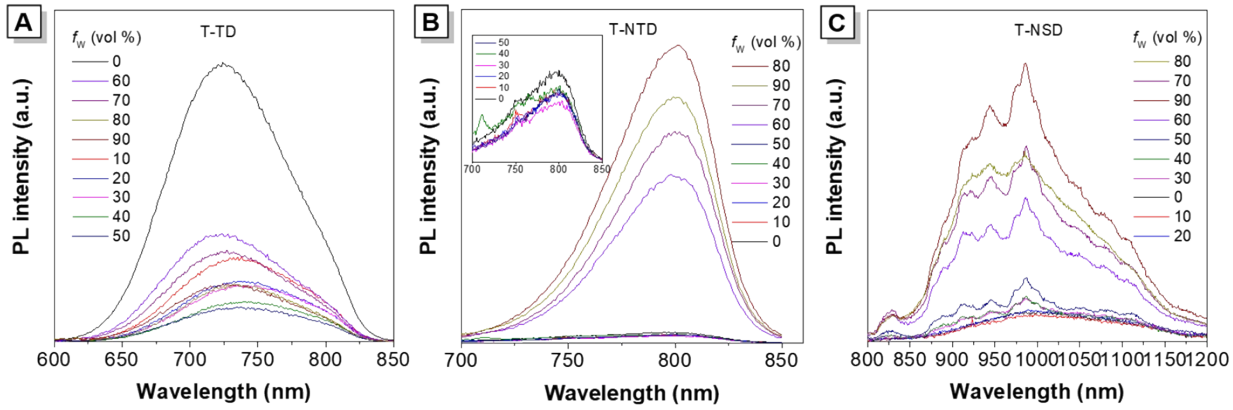

Figure S12. PL spectra of (A) T-BTD, (B) T-NTD and (C) T-NSD in THF/Water mixtures with different water fractions (f_w). Concentration: 10 μM.

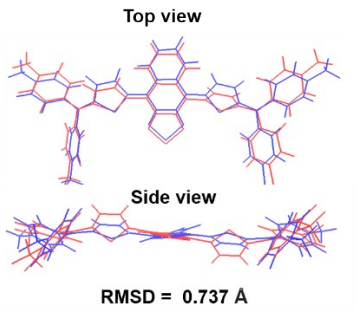

Figure S13. DFT minimum energy geometry of T-NSD calculated for the S_0 (black) and S_1 (red) electronics states.

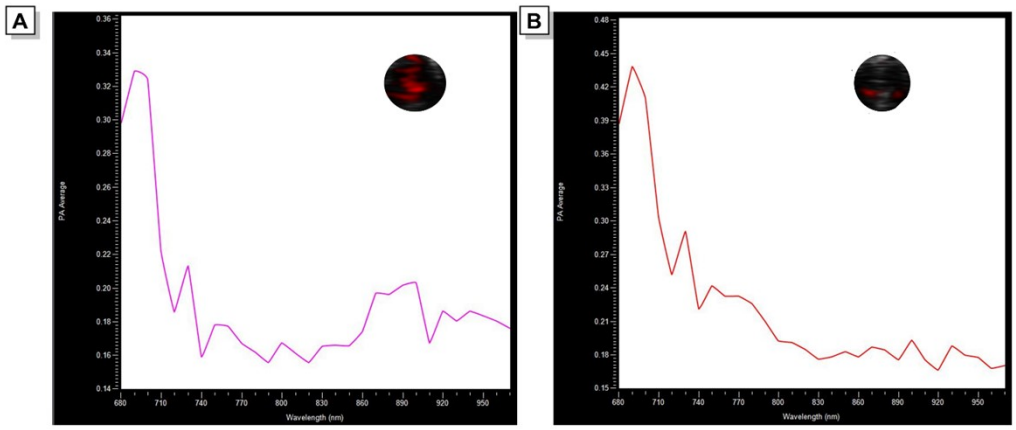

Figure S14. PA spectra of T-NSD in (A) aggregated state (f_w = 90%, 10 μM) and (B) solution state (THF, 10 μM).

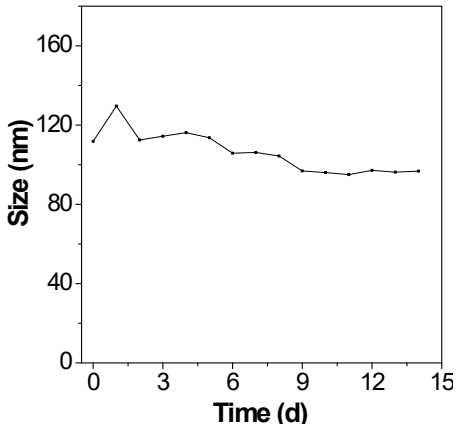

Figure S15. Size variations of T-NSD NPs in water during 7 days.

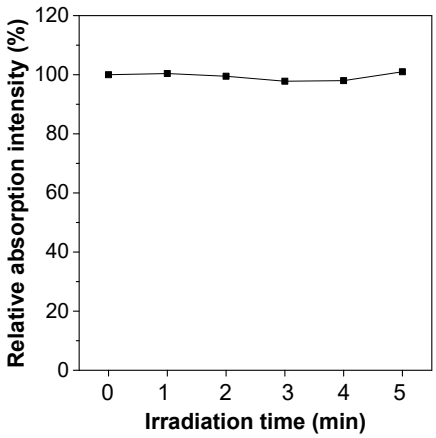

Figure S16. Absorption variations of T-NSD NPs (10 μM) as a function of irradiation time measured by UV–Vis–NIR spectrometer. Laser, 660 nm, 0.1 W cm^{-1}.

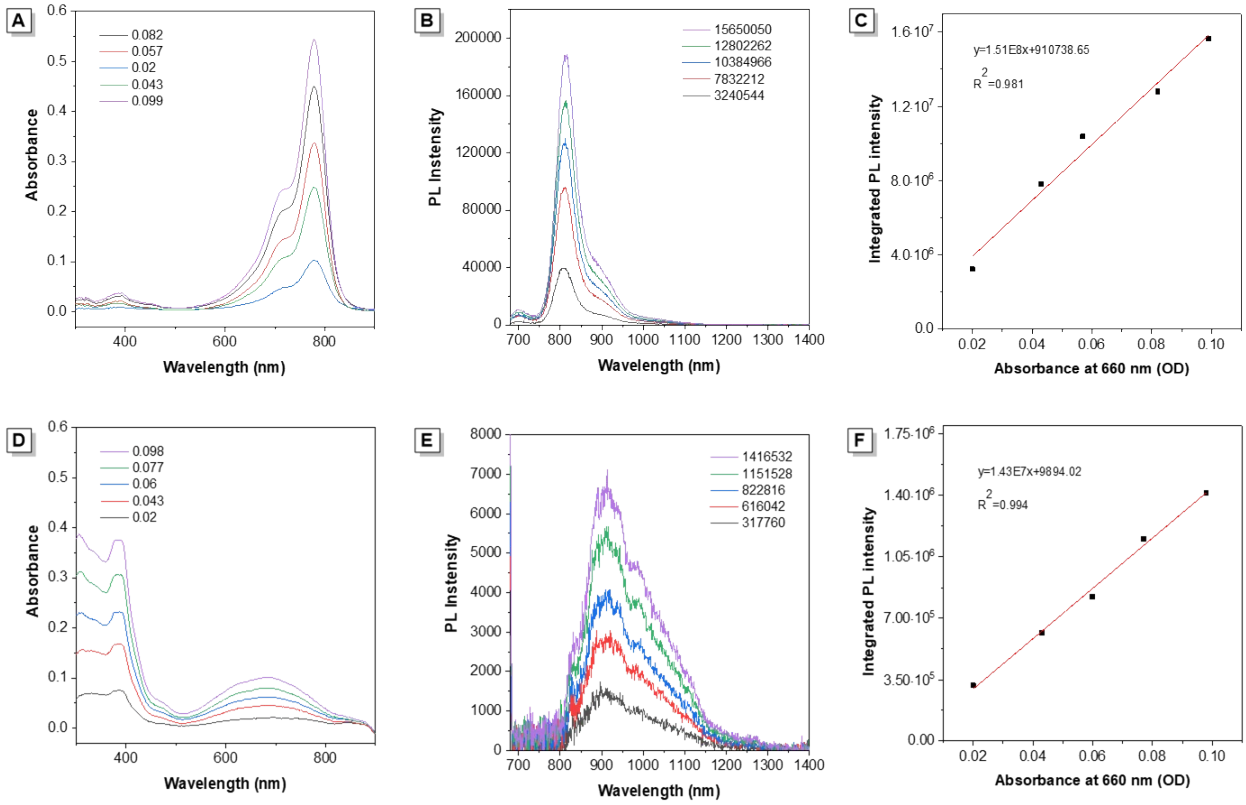

Figure S17. Relative fluorescence quantum yield calculation. UV-Vis-NIR absorption spectra, PL spectra, and a plot of integrated fluorescence intensity versus the absorbance at 808 nm of (A, B, C) ICG and (D, E, F) T-NSD NPs in ultrapure water (QY_{ICG} =1.6% in water).

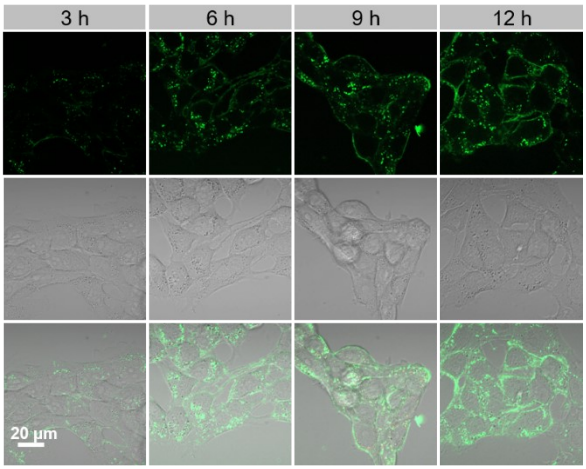

Figure S18. CLSM imaging of 4T1 cells incubated with FITC-NPs.

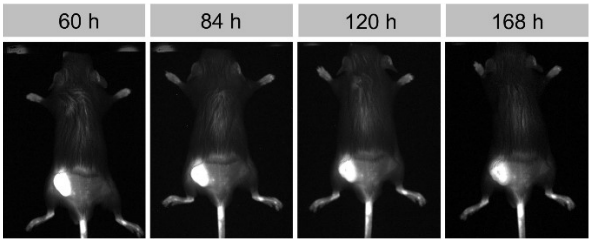

Figure S19. NIR-II fluorescence imaging on 4T1 tumor-bearing mice after injection of T-NSD NPs.

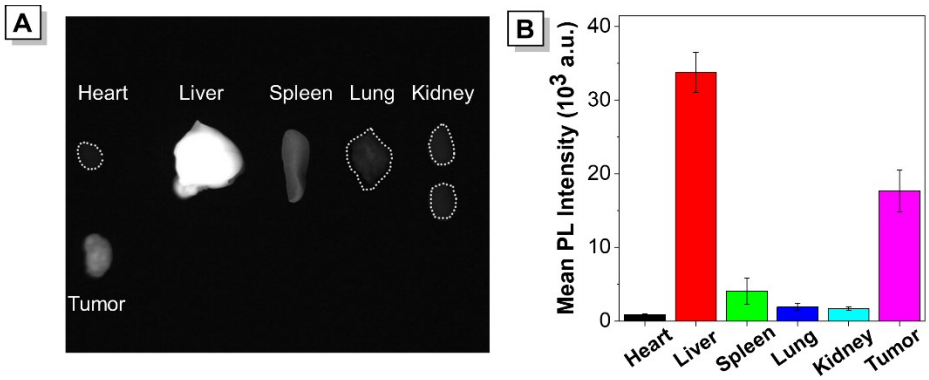

Figure S20. (A) Ex vivo NIR-II fluorescence images and (B) the corresponding mean fluorescence intensity of tumor and major organs after intravenous injection with T-NSD NPs for 36 h.

Table S1. Summary of the QYs of the three compounds T-BTD, T-NTD and T-NSD

Molecule	QYs (%) in THF solution	QYs (%) as nanoparticles
T-BTD	12.7	0.3
T-NTD	0.4	0.8
T-NSD	0.039[a]	0.15[a]

[a]Relative quantum yield measured by using ICG as reference (QY_{ICG} =1.6% in water)

Table S2. Routine blood analysis

Parameters	Unit	PBS	T-NSD NPs	Reference Range
WBC	10^9/L	6.7±0.7	6.6±0.01	0.8-10.6
Lymph	10^9/L	4.3±0.1	4.9±0.2	0.6-8.9
Mon	10^9/L	0.2±0.08	0.2±0.01	0.04-1.4
Gran	10^9/L	0.5±0.1	1.5±0.2	0.23-3.6
RBC	10^{12}/L	7.5±1.3	8.5±0.2	6.5-11.5
HGB	g/L	122.7±15.3	126.7±1.5	110-165
HCT	%	43.8±1.4	39.8±0.55	35-55
MCV	Fl	54±2.6	47±0.72	41-55
MCH	Pg	16.8±0.5	14.9±0.23	13-18
MCHC	g/L	324.3±4.6	317.3±1.6	300-360
RDW	%	16.3±2.5	14.3±0.35	12-19
PLT	10^9/L	853±105.7	833±45.7	400-1600
MPV	fL	5.3±0.7	7.03±0.06	4.0-6.2
PDW		15.3±0.01	17.2±0.01	12.0-17.5
PCT	%	0.63±0.5	0.59±0.4	0.100-0.780

References

1 W. Xu, Z. Zhang, M. Kang, H. Guo, Y. Li, H. Wen, M. M. S. Lee, Z. Wang, R. T. K. Kwok, J. W. Y. Lam, K. Li, L. Xi, S. Chen, D. Wang, B. Z. Tang, *ACS Materials Lett.,* 2020, **2**, 1033-1040.

2 Z. Shuai, *Chin. J. Chem.,* 2020, **38**, 1223-1232.

3 Z. Shuai, Q. Peng, *Phys. Rep.,* 2014, **537**, 123-156.

4 Z. Shuai, Q. Peng, *Natl. Sci. Rev.,* 2017, **4**, 224-239.

5 M. J. Frisch, G. W. Trucks, H. B. Schlegel, G. E. Scuseria, M. A. Robb, J. R. Cheeseman, G. Scalmani, V. Barone, G. A. Petersson, H. Nakatsuji, X. Li, M. Caricato, A. V. Marenich, J. Bloino, B.

G. Janesko, R. Gomperts, B. Mennucci, H. P. Hratchian, J. V. Ortiz, A. F. Izmaylov, J. L. Sonnenberg, D. Williams-Young, F. Ding, F. Lipparini, F. Egidi, J. Goings, B. Peng, A. Petrone, T. Henderson, D. Ranasinghe, V. G. Zakrzewski, J. Gao, N. Rega, G. Zheng, W. Liang, M. Hada, M. Ehara, K. Toyota, R. Fukuda, J. Hasegawa, M. Ishida, T. Nakajima, Y. Honda, O. Kitao, H. Nakai, T. Vreven, K. Throssell, J. A. Montgomery, Jr., J. E. Peralta, F. Ogliaro, M. J. Bearpark, J. J. Heyd, E. N. Brothers, K. N. Kudin, V. N. Staroverov, T. A. Keith, R. Kobayashi, J. Normand, K. Raghavachari, A. P. Rendell, J. C. Burant, S. S. Iyengar, J. Tomasi, M. Cossi, J. M. Millam, M. Klene, C. Adamo, R. Cammi, J. W. Ochterski, R. L. Martin, K. Morokuma, O. Farkas, J. B. Foresman, and D. J. Fox, *Gaussian 16*, Gaussian, Inc., Wallingford CT, 2016.